

Relativistic random-phase approximation longitudinal response functions for quasielastic electron scattering with nonlinear models

J. C. Caillon, P. Gabinski, and J. Labarsouque

Centre d'Etudes Nucléaires de Bordeaux-Gradignan,* Université Bordeaux I, IN2P3, Le Haut Vigneau, BP 120, F-33175 Gradignan Cedex, France

(Received 13 July 2000; published 24 January 2001)

The longitudinal response functions for quasielastic electron scattering on ^{12}C , ^{40}Ca , and ^{56}Fe have been calculated taking into account relativistic RPA correlations. For these calculations relativistic nonlinear models, providing a good description of ground state properties of finite nuclei, have been used. The effect of the nonlinear terms on the longitudinal response has been discussed.

DOI: 10.1103/PhysRevC.63.028201

PACS number(s): 21.65.+f, 12.40.-y, 21.60.Jz, 25.30.Bf

Since the original Walecka model [1], relativistic mean field models have been considerably improved and provide a rather good description of nuclear matter and ground state properties of finite nuclei [1–4]. In these models the nucleons interact self-consistently through meson field exchange in mean field approximation. The improved versions of the Walecka model, the so-called nonlinear models, include linear nucleon-meson couplings in the Lagrangian as well as couplings between the mesonic fields. Among many models, the models NL1 [5] and NL-SH [6] contain only σ self-coupling terms in the Lagrangian while TM1 (for medium and heavy nuclei) and TM2 [7] (for light nuclei) include in addition an ω self-coupling term in order to reduce the resulting strong scalar and vector potentials obtained with NL1 and NL-SH. More recently, two parameter sets $G1$ and $G2$ [8], coming from an effective field theory which allows all scalar-vector coupling terms up to fourth order in the Lagrangian, have been proposed. In the same work [8], another parameter set, $Q2$, retaining only the same terms as TM1 and TM2 is also given. All of these models lead to results which compare extremely well with the ground state properties of finite nuclei.

In a previous work [9], using the generating functional method, we determined the in-medium propagators of the σ and ω mesons in many nonlinear models. As an application of this formalism, the scalar and vector collective modes and the density dependence of the ω meson mass were considered. Since these collective modes happen in the timelike region, the question now arises for finding an observable that can characterize meson propagation in the spacelike region. A probe able to explore this region is quasielastic electron scattering. Indeed, quasielastic electron scattering is a powerful tool for exploring the meson propagation since the inclusive electron scattering differential cross section can be written in terms of the polarization tensor directly obtained from meson propagators.

In this work, we have determined the longitudinal response functions for ^{12}C , ^{40}Ca , and ^{56}Fe at a three-momentum transfer of 570 MeV/c taking into account relativistic random phase approximation (RPA) correlations. As

is well known, the longitudinal response functions can be written in terms of the polarization tensor. This polarization tensor has been obtained using many nonlinear models. Thus, an infinite sum of particle-hole excitations (in both isoscalar and isovector channels) as well as contributions coming from nonlinear terms have been taken into account in the determination of the response functions. Our results will be compared to the longitudinal response functions obtained by Jourdan [10]. The purpose of this work is not an accurate comparison of our results with the data (where large uncertainties exist especially at large energy transfer), but rather a comparison between the results provided by the different nonlinear models.

As is well known, the longitudinal response function can be written in terms of the polarization tensor $\Pi^{\mu\nu}$ (which is defined as the ground-state expectation value of a time-ordered product of nuclear currents J^μ and J^ν). Since the electromagnetic baryon current operator has been decomposed into isoscalar and isovector contributions, the response function can be written [11]

$$R_L(\omega, \|\mathbf{q}\|) = -\frac{1}{\pi} \text{Im}\{\Pi_{is}^{00}(\omega, \|\mathbf{q}\|) + \Pi_{iv}^{00}(\omega, \|\mathbf{q}\|)\}. \quad (1)$$

In order to obtain longitudinal response functions for finite systems we will use here the local density approximation such that the response of a nucleus is the sum of the responses of its volume elements treated as nuclear matter with local Fermi momenta $k_{Fp}(r)$, $k_{Fn}(r)$, and local effective nucleon mass $M_N^*(r)$. In the framework of the local density approximation, the relativistic RPA longitudinal response function for finite nuclei (with Z protons and N neutrons) is given by

$$R_L(\omega, \|\mathbf{q}\|) = 4\pi \int r^2 \left(\frac{-1}{\pi} \right) \left[\frac{Z}{A} \text{Im}\Pi_L(k_{Fp}(r), M_N^*(r); \omega, \|\mathbf{q}\|) + \frac{N}{A} \text{Im}\Pi_L(k_{Fn}(r), M_N^*(r); \omega, \|\mathbf{q}\|) \right] dr, \quad (2)$$

with $\Pi_L = \Pi_{is}^{00NM} + \Pi_{iv}^{00NM}$ where $\Pi_{is}^{\mu\nu NM}$ and $\Pi_{iv}^{\mu\nu NM}$ are the isoscalar and isovector parts of the polarization tensor in nuclear matter. The nuclear pointlike proton distributions required in the present analysis have been deduced, after the

*Affiliated with CNRS as UMR 5797.

proton finite-size correction has been made, from the electron scattering charge densities of Sick and McCarthy [12] for ^{12}C , Frosch *et al.* [13] for ^{40}Ca and ^{56}Fe .

Moreover, due to the separation of the current operator in Dirac and Pauli parts, each isoscalar and isovector contribution to the polarization tensor can be written as a sum of four contributions: a purely vector piece (VV), a purely tensor piece (TT), and two interference terms (VT and TV), such that

$$\begin{aligned} \Pi_{is}^{\mu\nu NM} = & F_{1 is}^2 \bar{\Pi}_{VV is}^{\mu\nu} + F_{1 is} F_{2 is} (\bar{\Pi}_{VT is}^{\mu\nu} + \bar{\Pi}_{TV is}^{\mu\nu}) \\ & + F_{2 is}^2 \bar{\Pi}_{TT is}^{\mu\nu}, \end{aligned} \quad (3)$$

$$\begin{aligned} \Pi_{iv}^{\mu\nu NM} = & F_{1 iv}^2 \bar{\Pi}_{VV iv}^{\mu\nu} + F_{1 iv} F_{2 iv} (\bar{\Pi}_{VT iv}^{\mu\nu} + \bar{\Pi}_{TV iv}^{\mu\nu}) \\ & + F_{2 iv}^2 \bar{\Pi}_{TT iv}^{\mu\nu}. \end{aligned} \quad (4)$$

For all of the models considered (NL1, NL-SH, TM1, TM2, Q_2 , G_1 , and G_2), the part of the Lagrangian density which will contribute to the scalar and vector meson propagation in symmetric nuclear matter reads

$$\begin{aligned} \mathcal{L} = & \bar{\psi} \left[\gamma_\mu (i\partial^\mu - g_{\omega 1} V^\mu - g_\rho \rho^\mu) - (M_N - g_{\sigma 1} \phi) \right. \\ & \left. - \frac{f_\rho}{4M_N} \rho_{\mu\nu} \sigma^{\mu\nu} - \frac{f_\omega}{4M_N} F_{\mu\nu} \sigma^{\mu\nu} \right] \psi + \frac{1}{2} (\partial_\mu \phi \partial^\mu \phi \\ & - m_\sigma^2 \phi^2) + \frac{1}{2} m_\omega^2 V_\mu V^\mu - \frac{1}{4} F_{\mu\nu} F^{\mu\nu} + m_\rho^2 \text{Tr}(\rho_\mu \rho^\mu) \\ & - \frac{1}{2} \text{Tr}(\rho_{\mu\nu} \rho^{\mu\nu}) - \frac{1}{3} g_{\sigma 3} \phi^3 + \frac{1}{3} g_{\sigma\omega 3} \phi V_\mu V^\mu - \frac{1}{4} g_{\sigma 4} \phi^4 \\ & + \frac{1}{4} g_{\omega 4} (V_\mu V^\mu)^2 + \frac{1}{4} g_{\sigma\omega 4} \phi^2 V_\mu V^\mu, \end{aligned} \quad (5)$$

where M_N is the nucleon mass, m_σ and m_ω , m_ρ the scalar and vector meson masses, and, as usual $F_{\mu\nu} = \partial_\mu V_\nu - \partial_\nu V_\mu$ and $\rho_{\mu\nu} = \partial_\mu \rho_\nu - \partial_\nu \rho_\mu$.

Using the generating functional method, we have determined the in-medium propagators of the σ , ω , and ρ mesons. Their expressions can be found in Ref. [9]. The diagrammatic representation of Dyson equations (taking into account an infinite sum of polarization insertions) is shown in Fig. 1(a). As already mentioned, the polarization operators include particle-hole excitations as well as contributions coming from nonlinear terms in the Lagrangian (except for the ρ meson). The full lines in Fig. 1 represent the in-medium nucleon propagator in which the nucleon self-energy includes linear as well as nonlinear terms (taken into account through the nucleon effective mass), while the dashed lines represent the mesons. The polarization tensor has been calculated using the in-medium meson propagators. The diagrammatic representation of $\bar{\Pi}_{ab is}^{\mu\nu}$ and $\bar{\Pi}_{ab iv}^{\mu\nu}$ in Eqs. (3) and (4) is then shown in Fig. 1(b).

We show in Figs. 2–5 the longitudinal response functions calculated with relativistic RPA correlations for ^{12}C , ^{40}Ca ,

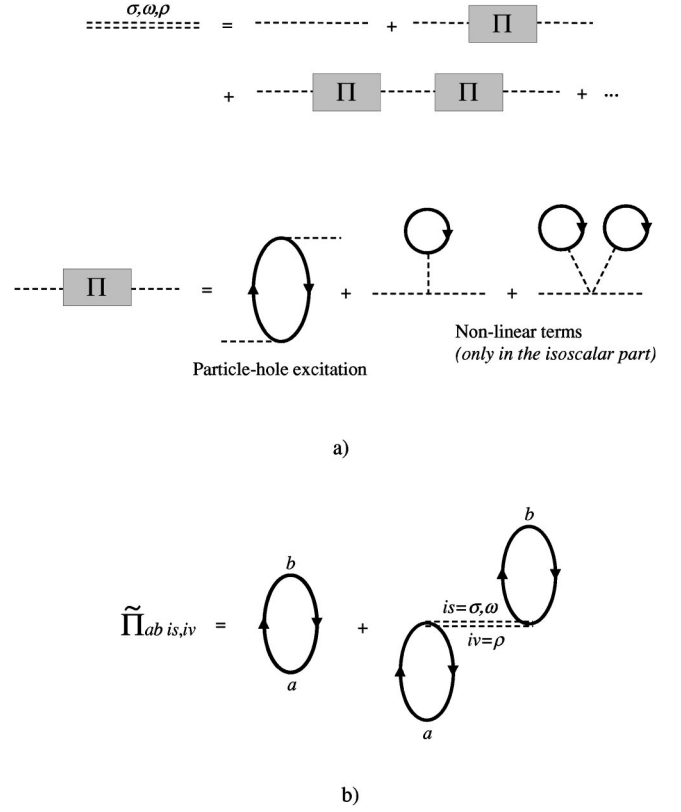


FIG. 1. The diagrammatic representation of the meson propagators is displayed in part (a). Part (b) shows the diagrammatic representation of the polarization tensor of nuclear matter.

and ^{56}Fe as a function of energy loss at a three-momentum transfer of 570 MeV/c. We have chosen a relatively high three-momentum transfer since previous calculations suggest that contributions from final-state interactions should vanish at sufficiently high $|q^2|$. Our results will be compared to the response functions obtained by Jourdan [10] using the “world data” on inclusive quasielastic scattering.

First, we have studied the influence of both relativistic RPA correlations and nonlinear terms on the longitudinal

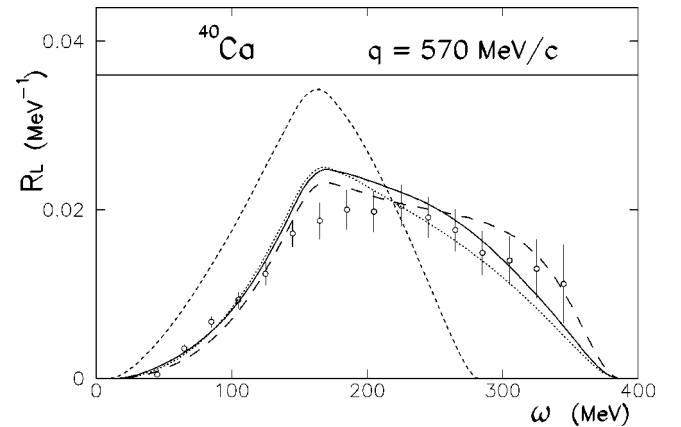


FIG. 2. Longitudinal response function for ^{40}Ca as a function of energy transfer for a three-momentum transfer of 570 MeV/c (see text). The experimental data are taken from Ref. [10].

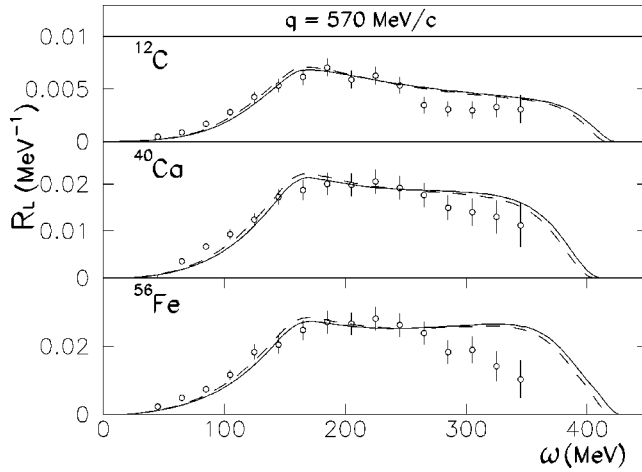


FIG. 3. Longitudinal response functions for ^{12}C , ^{40}Ca , and ^{56}Fe as a function of energy transfer ω for a three-momentum transfer of 570 MeV/c. The solid curves have been obtained by taking into account relativistic RPA correlations using the NL1 model while for the dashed curves we have used the NL-SH model. The experimental data are taken from Ref. [10].

response. In Fig. 2, the short-dashed curve is obtained with a simple Fermi gas model without any adjusted parameters. The solid curve represents a calculation taking into account relativistic RPA correlations obtained with the $G1$ model while for the dotted curve the $G1$ model is used but without relativistic RPA correlations (the dotted curve represents in fact the result of a Fermi gas calculation where the nucleon effective mass obtained in the $G1$ model has been used). As can be seen in Fig. 2, this curve is very close to the solid one obtained with the full $G1$ model. Thus, the effect of relativistic RPA correlations is found to be small with the $G1$ model for this high momentum transfer and a great part of the response is given by the use of the appropriate nucleon effective mass. The long-dashed curve represents the longitudinal response calculated with the $G1$ model in which only

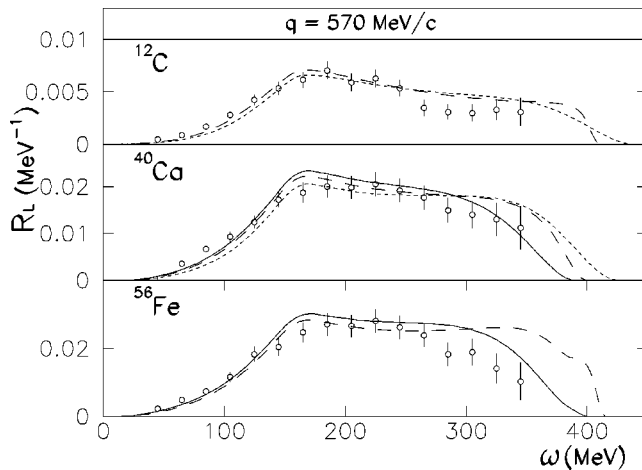


FIG. 4. Same as Fig. 3 but here the solid and short-dashed curves have been obtained, respectively, with the TM1 and TM2 models while for the long-dashed curves we have used the $Q2$ model.

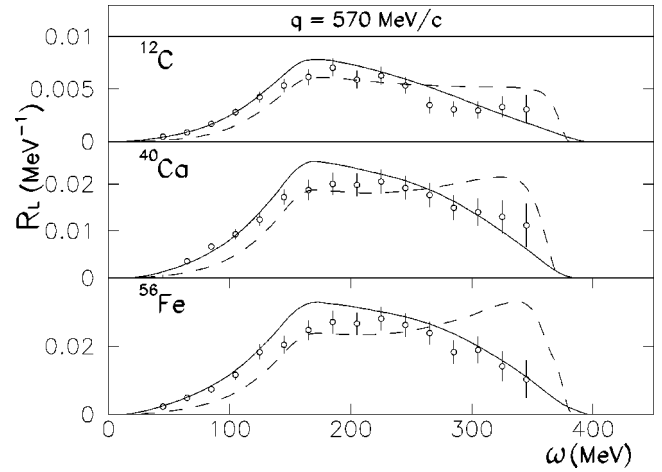


FIG. 5. Same as Fig. 3 but here the solid curves have been obtained with the $G1$ model while for the dashed curves we have used the $G2$ model.

the effects of the nonlinear terms have been omitted. In the very first place, the effects of the nonlinear terms can be seen relatively small since the long-dashed curve is close to the one obtained with the full $G1$ model. However, note that the effects of nonlinear terms are also to change the nucleon effective mass as well as the coupling constants of the linear couplings. For example, we have verified that the longitudinal response obtained with the $G1$ model without the nonlinear terms contribution strongly differs from the one given in the Walecka model which does not contain any nonlinear term, showing that the influence of these terms is not so small.

In Fig. 3 we show the results for very simple nonlinear models in which only the σ self-coupling terms in the Lagrangian are taken into account. The solid curves have been obtained with the NL1 model [5] while for the dashed curves the NL-SH model [6] has been used. As we can see, the longitudinal response functions are not very different from one model to another and give suitable agreement with the data. However, for high energy transfers we overestimate the response especially for ^{40}Ca and ^{56}Fe .

In Fig. 4, some more elaborated nonlinear models have been considered including in addition an ω self-coupling term in the Lagrangian. The solid and short-dashed curves have been obtained, respectively, with the TM1 (for $Z \geq 20$) and TM2 (for $Z \leq 20$) models [7] while for the long-dashed curves the $Q2$ model [8] has been used. Here the results obtained with TM1 and TM2 are in better agreement with the data than the ones obtained with the $Q2$ model, especially at large energy transfer.

In Fig. 5, we have used recent models which allow all scalar-vector coupling terms up to fourth order in the Lagrangian. The solid and the dashed curves have been obtained, respectively, with the $G1$ and $G2$ models [8]. Although these two models provide practically the same description of the nuclear properties (same χ^2 for $G1$ and $G2$), they give very different longitudinal response functions. The $G1$ model gives a better agreement with the data

than the results obtained with the $G2$ model for all the nuclei considered. However, note that the height of the peak is slightly overestimated for the $G1$ model.

In this work, we have determined the relativistic RPA longitudinal response functions for quasielastic electron scattering using nonlinear models. Three nuclei have been considered, ^{12}C , ^{40}Ca , and ^{56}Fe , and we have chosen a relatively high three-momentum transfer, $570\text{ MeV}/c$, in order to reduce the contribution coming from final-state interactions. We have found that the nonlinear terms contribution seems rather weak on the final result but, since the nonlinear terms lead also to a change on the linear coupling constants, we concluded that their influence is not so small. Although all of

the nonlinear models used in this work lead to a rather good description of the nuclear properties, they give different results for the longitudinal response. Indeed, the longitudinal response obtained with the TM1 and $G1$ models are in fair agreement with the data while the results given by the other models are worse, especially for the $G2$ model where the agreement is bad in the whole range of energy transfer. Thus, even if there are some uncertainties in the experimental data, the longitudinal response function can be seen as a tool to distinguish realistic nonlinear models from nonrealistic ones.

The authors would like to thank Dr. J. Jourdan for providing them the numerical values of the response functions.

-
- [1] B. D. Serot and J. D. Walecka, *Adv. Nucl. Phys.* **16**, 1 (1986).
[2] P. G. Reinhard, *Rep. Prog. Phys.* **52**, 439 (1989).
[3] Y. K. Gambhir, P. Ring, and A. Thimet, *Ann. Phys. (N.Y.)* **198**, 132 (1990).
[4] B. D. Serot, *Rep. Prog. Phys.* **55**, 1855 (1992).
[5] P. G. Reinhard, M. Rufa, J. Maruhn, W. Greiner, and J. Friedrich, *Z. Phys. A* **323**, 13 (1986).
[6] M. M. Sharma, M. A. Nagarajan, and P. Ring, *Phys. Lett. B* **312**, 377 (1993).
[7] Y. Sugahara and H. Toki, *Nucl. Phys.* **A579**, 557 (1994).
[8] R. J. Furnstahl, B. D. Serot, and H.-B. Tang, *Nucl. Phys.* **A615**, 441 (1997).
[9] J. C. Caillon and J. Labarsouque, *Phys. Rev. C* **62**, 035201 (2000).
[10] J. Jourdan, *Nucl. Phys.* **A603**, 117 (1996).
[11] C. J. Horowitz and J. Piekarewicz, *Nucl. Phys.* **A511**, 461 (1990).
[12] I. Sick and J. S. McCarthy, *Nucl. Phys.* **A150**, 631 (1970).
[13] R. F. Frosch *et al.*, *Phys. Rev.* **174**, 1380 (1968).